Applied CO_2 flux to monitor natural emission from geothermal field, New Zealand.

Tsung-Han Jimmy Yang[1,2], Isabelle Chambefort[1], Michael Rowe[2], Agnes Mazot[1], Cynthia Werner[3], Tobias Fischer[4], Jun Seastres[5], Thomas Brakenrig[1], Nick Macdonald[1], Lauren Coup[1], Fiona Sander[1].

1 GNS Science, Wairakei research Centre, New Zealand.

2 School of Environment, University of Auckland, New Zealand.

3.Research Geologist (under GNS Science contract), New Plymouth, New Zealand.

4 Department of Earth and Planetary Sciences, University of New Mexico, Albuquerque, U.S.A.

5 Contact Energy Ltd, Private Bag 2001, Taupo 3352, New Zealand

Tyan870@aucklanduni.ac.nz

Keywords: *CO_2 flux, CO_2 emission, temporal and spatial variation, Taupo volcanic zone, Tauhara geothermal field, Wairakei geothermal field, Karapiti, Rotokawa geothermal field.*

ABSTRACT

Soil CO_2 flux measurements could be used in geothermal areas to constrain surface CO_2 emissions and to monitor degassing anomalies from volcanic, tectonic, or anthropogenic activities. However spatial and temporal variations in a utilised geothermal field are difficult to assess at a large scale due to the prerequisite of a lengthy CO_2 flux survey and lack of monitoring data outside the power stations.

In this study, we analyse the temporal and spatial variations of soil CO_2 flux and soil temperature in the Taupo region. Fortnightly monitoring between 2019 to 2022 at 8 stations across the Tauhara and Wairakei geothermal fields provide insight into changes of seasonal variations and geothermal activities. Carbon dioxide flux at 2 stations at Karapiti and 1 background site in the Wairakei geothermal field remain constant over the 2.5-year interval of monitoring. In contrast, CO_2 flux at the 5 stations at Crown Park in the Tauhara geothermal field fluctuated synchronously.

To understand the broader distribution of natural degassing and to compare the CO_2 flux over decades, we mapped the CO_2 at Karapiti, Wairakei geothermal field (2021, 2003, 2018) (n=123), “Ring of Fire”, Tauhara geothermal field (2006, 2022) (n=646), and Rotokawa geothermal field (2003, 2011, 2022) (n=380). Differences in the CO_2 flux distribution and total emission over a decade suggest possible changes to fluid pathways, permeability zones and/or reservoir conditions. The result gives important statistical insight into time constraints for future surface CO_2 surveys and monitoring strategy in the geothermal field.

1. INTRODUCTION

Geothermal power stations in the Taupo town region (Figure 1) accounts for 58% of the geothermal power generation nationwide (McLean and Richardson, 2021) and play an important role in decarbonizing New Zealand. Greenhouse gas emission as CO_2 equivalent from 6 power stations of Wairakei (Wairakei, Te Mihi, and Poihipi), Tauhara (Te Huka), and Rotokawa (Rotokawa and Nga Awa Purua) geothermal field in the Taupo add up to 497 to 566 ton per day ($t\ d^{-1}$) (McLean and Richardson, 2019; McLean et al., 2020; McLean and Richardson, 2021). However, little is known about seasonal and annual variations in CO_2 emissions from natural geothermal features (fumaroles, steaming ground, hot pools, and flux through soil). The emission of the power station is measured at a single point at the same location, whereas the natural flux is over an area with different spatial and time scales of fluctuation. Therefore, mapping and monitoring CO_2 flux and soil temperature at natural features will potentially help understand the spatial distribution and changes in reservoir condition after years of geothermal utilization.

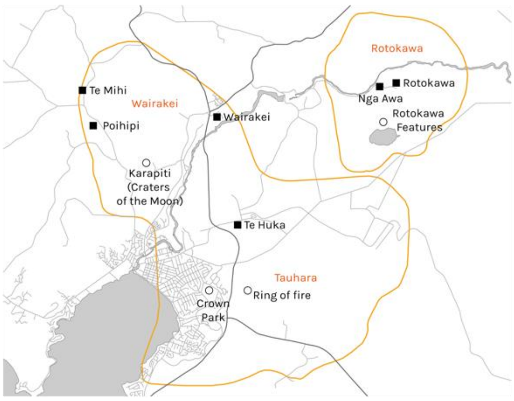

Figure 1: Regional map of Wairakei, Tauhara, and Rotokawa geothermal field. Geothermal field boundaries based on DC resistivity are marked by orange outline, power stations are marked by black squares, and the monitoring/mapping sites of natural geothermal features studied here are marked by open circles.

2. PROCESSES AFFECTING THE VARIABILITY OF SURFACE CO_2 FLUX

Surface CO_2 flux is driven by the concentration gradient between soil and air (diffusion) or fluid flow (advection), and therefore is influenced by the following processes that have been tested as part of this work:

1. **Soil temperature.** Fluids and heat are transported to the surface through hydrothermal convection (Henley and Ellis, 1983). Steaming ground with high CO_2 flux and high soil temperature is a common hydrothermal surface manifestation (Werner and Cardellini, 2006; Bloomberg et al., 2014; Harvey et al., 2018; Hughes et al., 2019).

2. **Permeability due to anthropological and natural processes.** Natural CO_2 in a geothermal field can originate from both magmatic degassing and biogenic sources. Fluids prefer a high permeability zone (Boseley et al., 2010;

Rissmann et al., 2012; Heap et al., 2017; Rosenberg et al., 2020) impacting where the CO_2 flux is distributed and how much CO_2 is emitted at the surface (Camarda et al., 2009; Ganot et al., 2014). Faults and lithologies control the permeability in a geothermal reservoir. Hydrothermal alteration and tectonic events can change the permeability pathway over time. Roads or construction may alter the surface permeability or result in lateral CO_2 flow.

3. **Seismic activity.** Both natural seismic events, and induced seismicity due to geothermal power station re-injection, occurs in the Taupo region (Bryan et al., 1999; Hopp et al., 2020). Faults and fractures can act as preferred fluid pathways for fluid migrating (Taussi et al., 2022) to the surface and seismicity can enhance fluid transport (Claesson et al., 2004; Yang et al., 2006; Fu et al., 2017).

4. **Seasonal variation.** Occurrence of seasonal temperature and precipitation cycle can influence the soil CO_2 flux (Delsarte et al., 2021). A low CO_2 flux is often observed during or after rain due to blocked or re-directed gas migration pathways (Boudoire et al., 2018). Air temperature and pressure variation can also significantly influence the CO_2 flux. The correction of the two parameters is explained in the method section.

5. **Soil type and vegetation.** The respiration of plant roots or biogenic CO_2 can alter the soil CO_2 flux observed at the surface (Wang et al., 2010).

6. **Utilizations of the field.** Pressure change in the reservoir can influence the surface CO_2 emission. The CO_2 emission from natural features compared with emission from geothermal power plants is reported in various studies (Hinkle, 1991; Ármannsson et al., 2005; Sbrana et al., 2021).

7. **Sampling and data statistics.** The selection of location controls the single point CO_2 flux monitoring result. CO_2 emission is calculated from combining multiple CO_2 flux points. Therefore, the gridding of the map and the interpolation method used also control the result aside from the factors listed above.

3. METHOD

3.1 Flux Measurement

Gas flux measurements of CO_2 and H_2S were realized using an accumulation chamber (Chiodini et al., 1998). We used the West System LICOR LI-820 infrared gas analyzer for CO_2 and TOX05 H_2S gas analyzer is used for H_2S (WestSystems, 2019). Ambient air pressure and temperature are measured during the flux survey for correlation of data. The flux is calculated following the equation below.

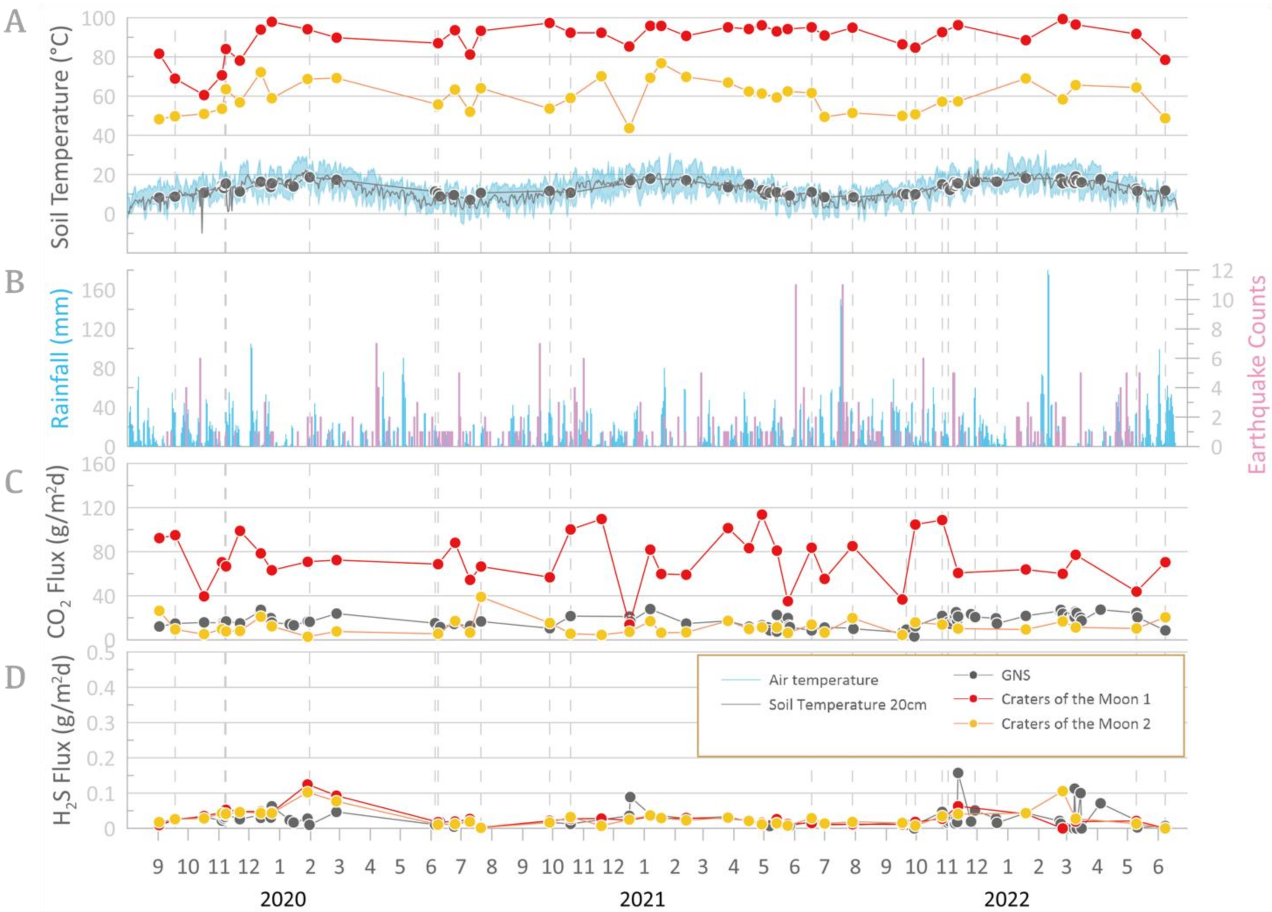

Figure 2: Karapiti monitoring measurements from September 2019 to June 2022, Y axis is (A) the soil temperature compared to The National Climate Database, 2022 (B) Accumulated rainfall (blue bar) (48hr rain fall>5mm marks as grey dashline) and earthquake counts (pink bar), (C) CO_2 flux, and (D) H_2S flux.

$$F_c = F_r*(P/10)/(101.3)*((298)/(T+273))* D_f$$

$$D_f = k*V/A$$

(F_c: Calculated Flux (g/m^2day), F_r: Raw Flux (ppm/s), P: Ambient air pressure (mbar), T: Ambient air temperature (°C), D_f: Dimension factor, k: Coefficient converting ppm/s to g/day, V: Total volume combining the chamber volume and the dead volume for the system (m^3), A: Area covered by the chamber (m^2))

3.2 CO_2 flux Map and CO_2 Emissions

We used a 25m grid-spacing for the CO_2 map in the geothermally active area and increased this to a 100m spacing where the CO_2 flux dropped to background levels defined by previous studies (Rissmann et al., 2012; Bloomberg et al., 2014). Carbon dioxide flux data were processed using WinGslib (Deutsch and Journel, 1998). The data were first processed with a normal score transformation so that the dataset conforms to a normal distribution for statistical analysis. A spherical variogram model is run to fit the normalized flux data. The data generated from the Sequential Gaussian Simulation (sGs) with 100 simulations were used for estimating the total CO_2 emissions from the lake using MATLAB.

4. RESULTS AND CASE STUDY

4.1 Short Term Effect: Fortnightly site monitoring at Wairakei and Tauhara geothermal fields.

The 3-year monitoring results from 2019-2022 of Karapiti (Wairakei geothermal field) and Crown Park (Tauhara geothermal field) are plotted in Figures 2 and 3, respectively.

A background monitoring site at GNS Wairakei Research Centre ranges from 3.1 to 27.9 g m^{-2} d^{-1} for CO_2 flux and 8.2 to 19.4 °C for soil temperatures at 15cm. H_2S flux from 8 monitoring stations in Figures 2 and 3 is below 0.2 g m^{-2} d^{-1}. The ground temperature variation for the GNS site is within the range of weather stations from both 20cm-ground-temperature (4.1 to 25.0°C) and air temperature (-5.6 to 32.5°C) during the three-year interval.

Two monitoring sites are located at Karapiti, both having an altered ground surface. Standard deviations are calculated to 1σ (Fig 2). CM1 has a mean CO_2 flux of 72.9 ± 22.8 g m^{-2} d^{-1}. The mean soil temperature of CM1 is 89.3 ± 8.7 °C. CM2 has a mean CO_2 of flux 11.9 ± 7.1 g m^{-2} d^{-1}. The mean soil temperature of CM2 is 59.6 ± 8.0 °C.

Five monitoring sites located at Crown Park, where CP1, CP2, CP3, CP4 are sitting on altered ground, and CP5 on short grass, were added to the monitoring suite in 2021 due to the observed surface anomalies from satellite image (Bromley et al., 2019). The highest CO_2 flux is observed at CP2 with a mean flux of 1405, σ=2315 g m^{-2} d^{-1} and a moderate to low soil temperature (mean 20.3, σ=4.4°C) (Figure 3). CP1 and CP4 have a similar mean CO_2 flux (998 and 1049 g m^{-2} d^{-1}) and mean soil temperature (80.8 and 84.8°C). CP3 and CP5 have a moderate to low CO_2 flux (75.5 and 66.5 g m^{-2} d^{-1}). CP3 has a soil temperature (mean 16.0, σ=5.2°C) within the range of air temperature variation whereas CP5 has soil temperature (mean 20.2, σ=4.9°C) similar to CP2, 5-10°C higher than the soil temperature at nearby the weather station.

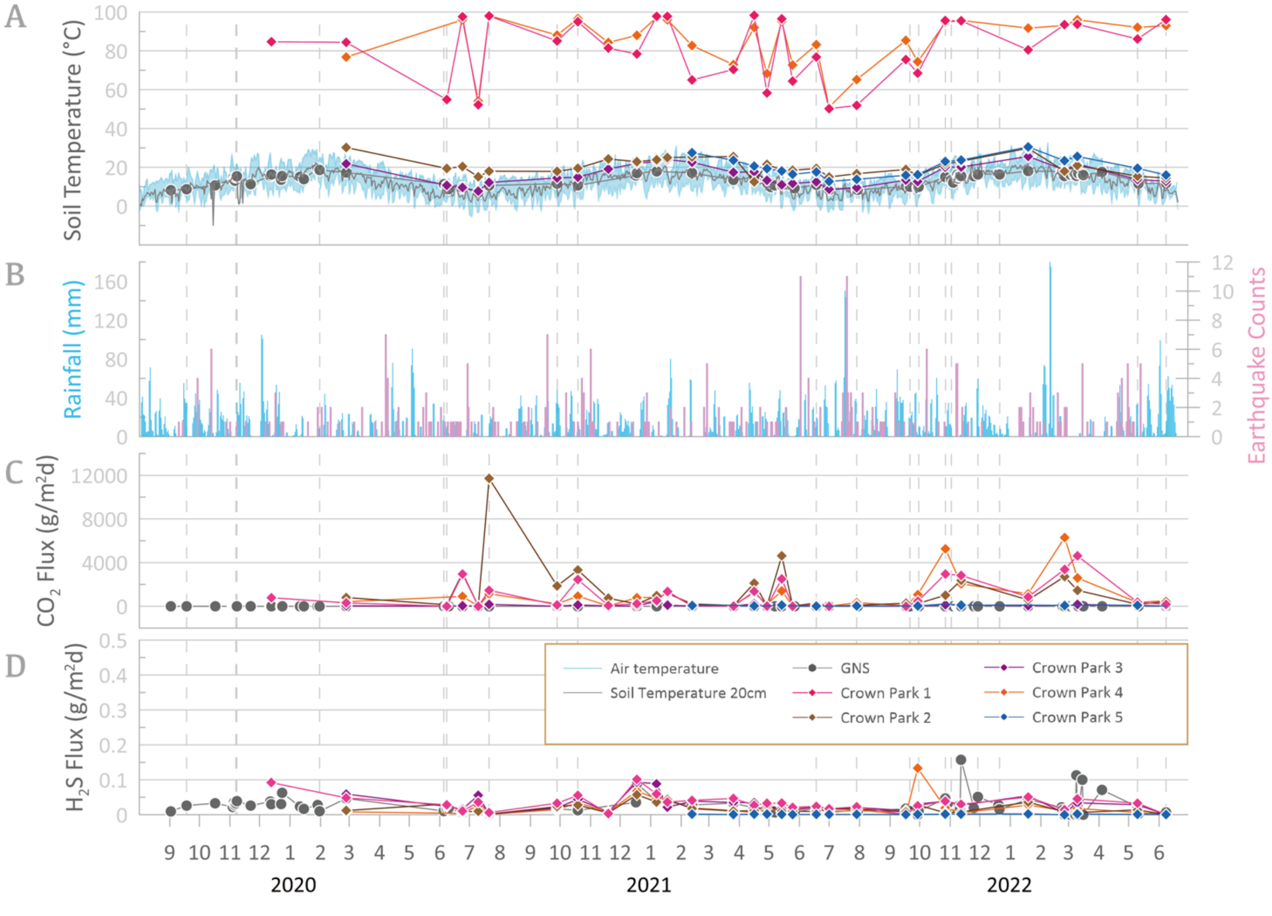

Figure 3: Crown Park monitoring measurements from September 2019 to June 2022, Y axis is (A) the soil temperature compared to The National Climate Database, (B) Accumulated rainfall (48hr rain fall>5mm marked as grey dashed line) and earthquake counts, (C) CO_2 flux, and (D) H_2S flux.

4.2 Long term effect: Comparing the CO_2 map across a decade.

Our CO_2 flux survey at Karapiti, Wairakei geothermal field (n=124) covers an area of 0.35 km^2 (Figure 4). High CO_2 flux is distributed at the southern part of the survey. Previous CO_2 flux surveys at Karapiti utilised the same equipment (West Systems flux meter) at the same area (Werner et al. 2004; Harvey et al., 2018). Diffusive emission was 6 t d^{-1} (tons per day) in 2004, 7.4 ± 0.6 t d^{-1} in 2018, and 19.9 ± 1.4 t d^{-1} in 2021 in this study.

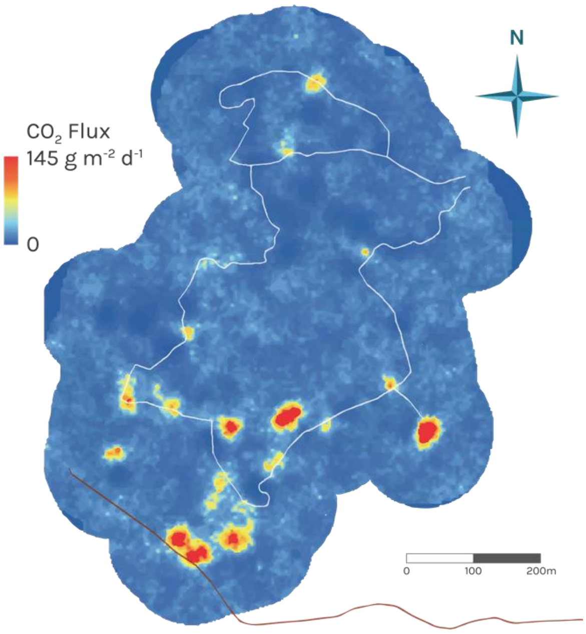

Figure 4: Gas flux survey at Karapiti between the 19 November 2020 and the 18 January 2021. The color scale ranges from 0 to 145 g m^{-2} d^{-1}. The white line marks the walking trail and the brown line marks the forestry road.

In 2006, a CO_2 flux survey (n=519) was completed at the Ring of Fire in the Tauhara geothermal field (Fig 5A). We mapped the same area and expanded the survey to cover 1.7 km^2 of area in 2021(n=646) (Fig 5B). In both maps, high CO_2 flux is observed mainly along the ring structure. The total CO_2 emission in 2021 is 109 ± 4.8 t d^{-1}. Among the overlapping areas between the 2021 and 2006 CO_2 flux maps (s.t. σ=8.5 g m^{-2} d^{-1}) 69% of the area (1.48km^2) has minor changes in CO_2 flux at less than1 σ, 17% of the area (0.36km^2) has an increasing CO_2 flux at more than 1 σ, and 14% of the area (0.31km^2) has a decreasing CO_2 flux by more than 1 σ. The total CO_2 emission of the overlapping area is 47.3 t d^{-1} in 2006, similar to the value of 48.5 t d^{-1} in 2021.

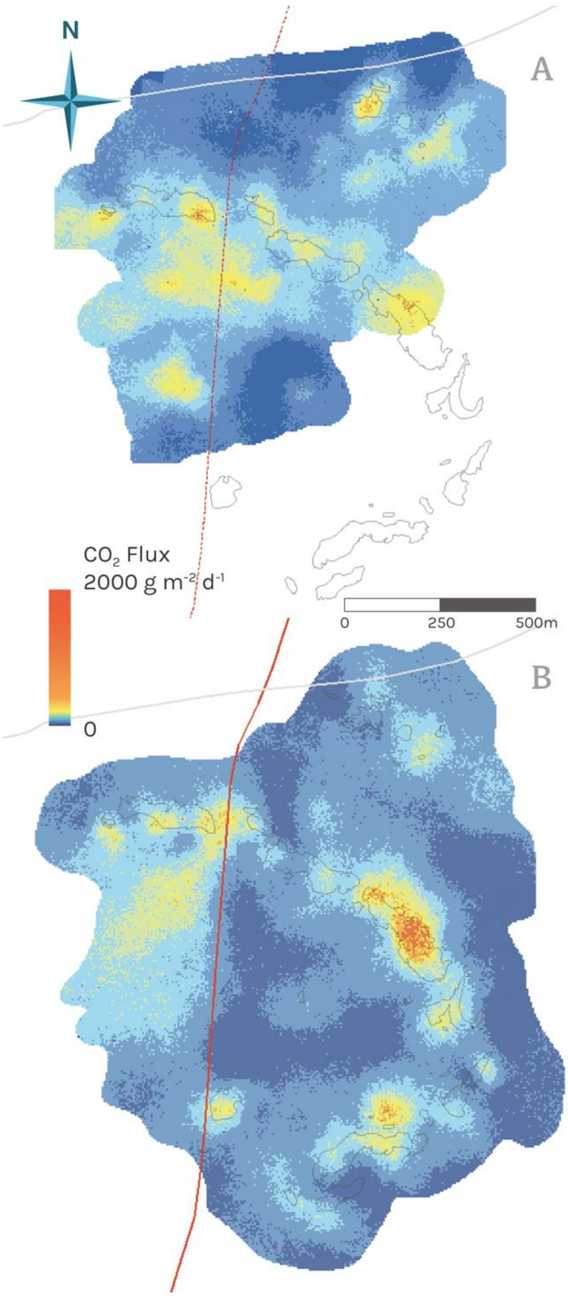

Figure 5: Gas flux survey at Ring of Fire (Tauhara) for 2006(A) and 2021(B). The CO_2 colour scale for both maps ranges from 0 to 2000 g m^{-2} d^{-1}. The grey polygon marks the ring shape of the geothermal surface features. The red line marks the state highway built after 2006, and the grey line marks Broadland Road.

Detailed CO_2 flux mapping of Rotokawa features (n=2500) was done between 2003-2011 (Bloomberg et al., 2014). In this study, we select 500 points from four different CO_2 flux ranges (<30, 30-100, 100-1000, and >1000 g m^{-2} d^{-1}) of the original data to be representative of the distribution and emission. The CO_2 emission over an area of 2.9 km^2 calculated from all 2500 points by Bloomberg et al., 2014 is 441±84 t d^{-1}. The CO_2 map from the 500 selected data points is shown in Figure 6A and the total emission re-calculated is 425±98 t d^{-1}. The same location is mapped again in March-July 2022. Among the 500 points, 380 were accessible for resampling as the topography and vegetation change, the new flux map is shown in Figure 6B. The original CO_2 flux versus the new CO_2 flux at the same location is plotted in Figure 6C. Moderate correlation is shown between the two time periods (R^2 = 0.53). Among the 380 repeated points in 2022, 130 points (34%) have variations less than an order of magnitude, 169 points (44%) decrease in CO_2 flux, and 81 points (21%) increase in CO_2 flux.

5. DISCUSSIONS AND IMPLICATIONS

Here we review the processes that affect the time variability of soil CO_2 flux for the short-term and long-term monitoring results.

1. **Soil temperature.** High CO_2 flux is often coupled with steaming ground and high soil temperature, but this is not always the case. The 8 short term monitoring stations (GNS, CM1, CM2, CP1, CP2, CP3, CP4, and CP5) can be divided into 4 categories as shown in Figure7:

(1) high CO_2 flux and high soil temperature - CM1, CP1, and CP4. CM1 shows very little change over the 3-year monitoring time in terms of CO_2 flux and soil temperature. CP1 and CP4 have a wide range of CO_2 flux and soil temperature and clear relationship between them (R^2= 0.70 for CP1 and R^2=0.56 for CP4; Fig 7).

(2) low CO_2 flux and low soil temperature - GNS, CP3 and CP5. The GNS site was design as a background site for the Taupo region. Soil temperature at GNS follows the ground temperature of the weather station, and the CO_2 flux is below 30 g m^{-2} d^{-1} though the 3-year time. CP3 provides a baseline for crown park, the soil temperature is 0-5°C higher than the normal soil temperature, the CO_2 flux is 1-3 order low then other monitoring station at Crown Park. Unlike CP1-4, CP5 is not located at geothermal altered ground. It has similar range of CO_2 flux and soil temperature as CP3 but has reasonably good correlation (R^2=0.50) between CO_2 flux and soil temperature such as CP1 and CP4.

(3) low CO_2 flux and high soil temperature - CM2. This may be caused by self-sealing at the geothermal area, resulting in low permeability (Facca and Tonani, 1967; Fulignati et al., 1996; Hochstein and Browne, 2000). Therefore, this may result in the blocking of the fluid passing through, while heat can still be conducted. This phenomenon is often observed in geothermal areas (Canet et al., 2010; Canet et al., 2015; Bolós et al., 2022).

(4) High CO_2 flux and low soil temperature - CP2. CP2 has the highest CO_2 flux measurements among all the monitoring stations, especially during August 2020 to October 2021. The soil temperature is only 0-10°C higher than the normal soil temperature. This can be explained by either condensation of vapor during fluid migration (Aubert, 1999) or is affected by undeveloped fractures that did not reach the surface (Giammanco et al., 2016).

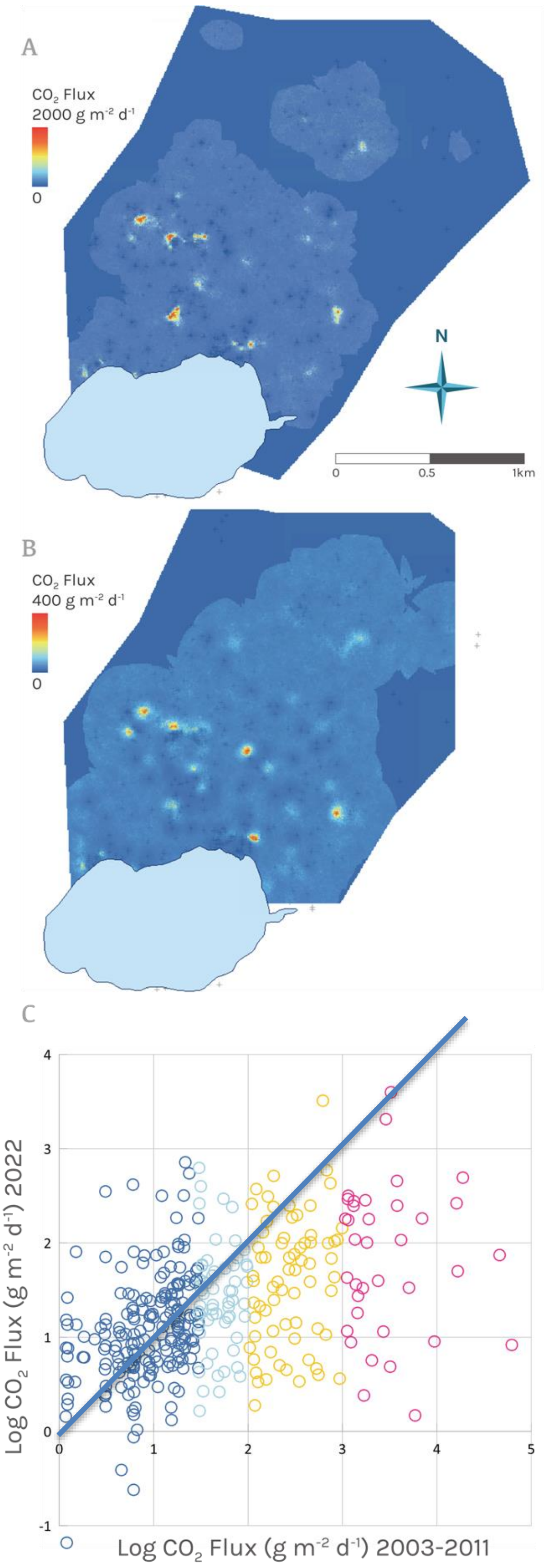

Figure 6: Gas flux survey at Rotokawa for (A)2003-2011 (n=500) and (B) 2022 (n=380). The light blue polygon marks the location of Lake Rotokawa. (C) Comparison between the log CO_2 flux of the two time periods. Colour scale represent four different CO_2 flux ranges (<30, 30-100, 100-1000, and >1000 g m^{-2} d^{-1}) of the original data (2003-2011).

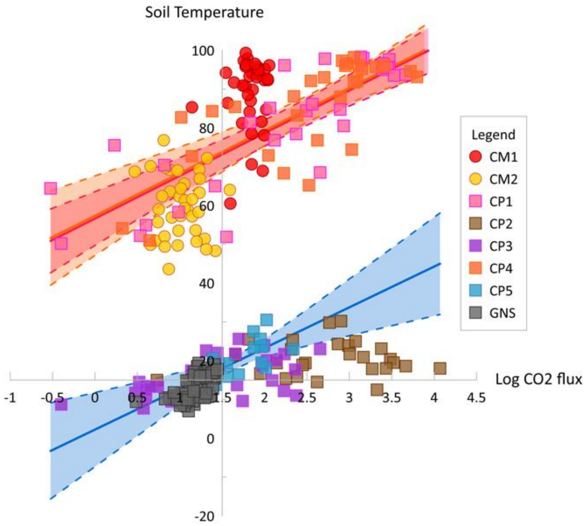

Figure 7: Log CO_2 flux (g m^{-2} d^{-1}) versus soil temperature at 15 cm depth (°C). Monitoring sites at Karapiti are marked as circle and monitoring sites at Crown Park are marked as square. Regression line and confidence interval of CP1, CP4, and CP5 is marked as solid and dash line, respectively.

2. **Permeability due to anthropological processed and natural process.** The Tauhara geothermal field's Ring of Fire provides an example of how human infrastructure modifies the distribution of CO_2 emissions. In 2006, before the state highway was built, high CO_2 flux was distributed following the ring features (Figure 5A).

Figure 8: Satellite images in 2006 and 2022 of the Ring of Fire, Tauhara geothermal field. The motor park decrease in size after the highway was built.

After the road was built, CO_2 anomalies decreased or were directed toward the SW at the junction of highway and ring features, this phenomenon is also observed at other sections of the state highway (Figure 5A). Although the distribution of CO_2 changes between 2006 and 2021 map, the total emission of the whole area is the same (47.3 t d^{-1} for 2006 and 48.5 t d^{-1} for 2021), indicating that the deep degassing remains constant as the surface pathways changes.

3. **Seismic activities.** 307 earthquakes occurred between September 2019 to May 2022 in the Taupo region. From the 3-year monitoring data, CM1 and CM2 however, have no CO_2 flux anomalies (Figure 2). High CO_2 peaks at Crown Park (Figure 3) measured on 06-2020, 07-2020, 10-2020, 04-2021, 05-2021, 10-2021, 02-2022, and 03-2022 do not match any of the high earthquake counts in Figure 3 or any earthquakes having magnitude higher than 3, suggesting that induced seismicity or natural seismic event does not affect the overall flux at the time scale of this study.

4. **Seasonal variation.** Variation in the Taupo region weather includes yearly temperature changes and wet/dry seasons. Most of the soil CO_2 measurements were performed during dry days or there were 3 days of dry weather before the measurement thus the effect of rainfall is negligible. No correlation was found (R^2<0.03) in our dataset between rainfall and CO_2 flux, the only strong decrease in soil CO_2 possibly related to rainfall is on 8th June 2020 with 9.8mm of rainfall 48hr before. For seasonal variations of soil temperature, the low temperature sites (CP2, CP3, and CP5) change together with the weather station temperature. The high temperature sites (CP1 and CP4) also saw influence from seasonal variation, having minimum soil temperatures of 50°C during June to August, and having maximum soil temperature of near boiling temperature 98°C in many other months (Figure 3).

5. **Soil type and vegetation.** CO_2 data is compared to ground and vegetation categories from Seward et al., 2018 in Figure 9. High CO_2 flux is observed near collapse craters with active fumaroles with bare ground or ground with low vegetation coverage. The CO_2 map in Figure 4 also shows wide CO_2 anomalies distributed to the S or SW of Karapiti, this matches the bare-ground surface/ low vegetation cover in Figure 9 and the thermal infrared image in Seward et al., 2018. Ground cover and vegetation height can be indicative of shallow soil temperatures (Given, 1980; Burns, 1997; Van Manen and Reeves, 2012) and CO_2 flux.

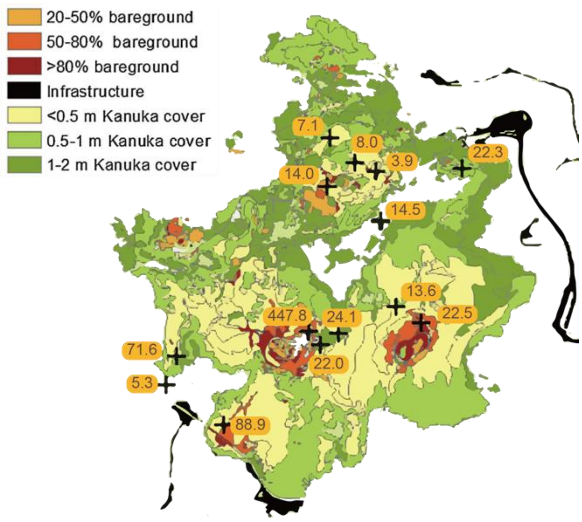

Figure 9: Vegetation cover classification for the Karapiti thermal area modified from Seward et al., 2018. CO_2 flux is marked in yellow text boxes in g $m^{-2}d^{-1}$.

6. **Utilization of the fields.** A trend in declining emission intensity has previously been reported for the Rotokawa, Ngatamariki, and Ngawha geothermal fields (Mclean and Richardson, 2019; Mclean et al., 2020; Mclean and Richardson, 2021). The Rotokawa field hosts both the Rotokawa and Nga Awa Purua (NAP) power plants. The data (from Mclean and Richardson, 2019; Mclean et al., 2020; Mclean and Richardson, 2021; NZGA, 2022) for the two power stations is plotted in Figure 10. From the repeating survey at the same location at the Rotokawa natural features (compared to Bloomberg et al, 2014, Figure 6), 44% of the points have decreasing CO_2 flux by more than an order of magnitude, more than twice the amount of increasing CO_2 flux points (21%). This decreasing flux is more notable for the high flux data in 2003-2011 (100-1000g m^{-2} d^{-1}, yellow circle, and >1000g m^{-2} d^{-1}, red circle in Figure 6.) However, more work needs to be carried out to confirm the decreasing trend of natural emission of the Rotokawa field including having at least 500 repeating points and calculating the total emission of the Rotokawa field in 2022.

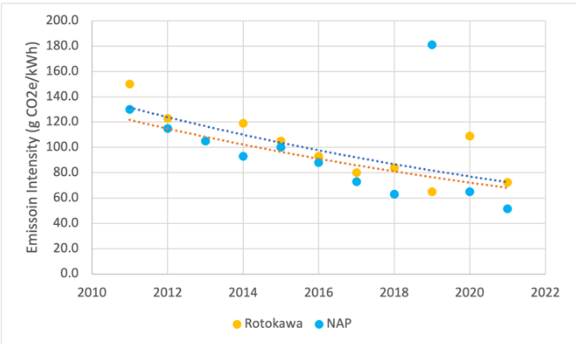

Figure 10: Emission intensity from Rotokawa and NAP power station from 2011 to 2021 (modified from Mclean and Richardson, 2019; Mclean et al., 2020; Mclean and Richardson, 2021; NZGA, 2022). Dashed lines are the exponential fitting lines of the trends.

7. **Sampling and data statistics.**

Short-term single point monitoring and long-term regional CO_2 maps takes years of surveying. For the former, the interval of sampling time determines the resolution of the results (fortnightly for this study). For the latter, the space gridding (25-100m is used for different areas in this study) and the location determines the confidence interval of unknown interpreted points. The method of interpolating also has influence on the calculation of total emission.

6. CONCLUSION

Fortnightly soil CO_2 flux monitoring coupled with soil temperature measurements over 3 years in the Wairakei and Tauhara geothermal field provide a detail analysis to identify the control on degassing in geothermal area. CO_2 flux and soil temperature are generally stable at Karapiti over the 3-year monitoring period. CO_2 flux at all sites of Crown Park vary together, while the soil temperature can be divided into high and low temperature groups, both vary with yearly temperature variations.

Repeated CO_2 flux surveys in the same area enable understanding of the spatial CO_2 redistribution, recalculation of the CO_2 flux, and (re)estimation of total CO_2 emission from the field. Karapiti in the Wairakei geothermal field has CO_2 anomalies distributed at the S/SW of the area. The emission changes from 6 t d^{-1} in 2004 to 7.4 t d^{-1} in 2018 and to 19.9 t d^{-1} in 2021. The Ring of Fire in the Tauhara geothermal field has major changes of CO_2 flux distribution due to infrastructure but the total emission of the overlapping area remains the same between 2006 (47.3 t d^{-1}) and 2021 (48.5 t d^{-1}). The total CO_2 emission of the feature in Tauhara field is 109 t d^{-1}. On land geothermal features (n=380) at the Rotokawa geothermal field were resampled at the same locations to compare the time variation of CO_2 emission between 2003-2011 and 2022. 44% of CO_2 flux measurements decreased for natural features, in accordance with the observed decreasing trends at the two power stations of Rotokawa geothermal field.

ACKNOWLEDGEMENTS

This work is supported by the Royal Society of New Zealand Marsden Fund to IC (18-GNS-022) “Superhot fluids: The origin and flux of natural greenhouse gases in volcanic areas”. T. J. Yang would like to acknowledge the Taiwanese Government and the University of Auckland for scholarship support. We would like to thank the Tauhara Moana Trust and Tauhara Mountain Trust for support in accessing the natural features in the Tauhara geothermal field as well as Contact Energy. We thank Mercury, the Department of Conservation, Ngati Whaua and Tuwharetoa Trust for access to Rotokawa geothermal features. We also acknowledge the New Zealand GeoNet project and its sponsors Earthquake Commission (EQC), GNS Science, and Land Information New Zealand (LINZ), the National Emergency Management Agency (NEMA) and the Ministry of Business, Innovation and Employment (MBIE) with Geonet for providing the past CO_2 flux data for Tauhara geothermal field.

REFERENCES

Aubert, M. (1999) Practical evaluation of steady heat discharge from dormant active volca-noes: case study of Vulcarolo fissure (Mount Etna, Italy). Journal of Volcanology and Geothermal Research, 92, 413-429.

Bloomberg, S., Werner, C., Rissmann, C., Mazot, A., Horton, T., Gravley, D., Oze, C. (2014) Soil CO_2 emissions as a proxy for heat and mass flow assessment, Taupō Volcanic Zone, New Zealand. Geochemistry, Geophysics, Geosystems, 15, 4885-4904. https://doi.org/10.1002/2014GC005327.

Bolós, X., del Ángel, V., Villanueva-Estrada, R. E., Sosa-Ceballos, G., Boijseauneau-López, M., Méndez, V., Macías, J. L. (2022) Surface hydrothermal activity controlled by the active structural system in the self-sealing geothermal field of Acoculco (Mexico). Geothermics, 101, 102372. https://doi.org/10.1016/J.GEOTHERMICS.2022.102372

Boseley, C., Cumming, W., Urzúa-monsalve, L., Powell, T., Grant, M. (2010) A resource conceptual model for the Ngatamariki geothermal field based onrecent exploration well drilling and 3D MT resistivity imaging. In: WorldGeothermal Congress, vol. 4, Bali, Indonesia.

Boudoire, G., Finizola, A., di Muro, A., Peltier, A., Liuzzo, M., Grassa, F., Delcher, E., Brunet, C., Boissier, P., Chaput, M., Ferrazzini, V., Gurrieri, S. (2018). Small-scale spatial variability of soil CO_2 flux: Implication for monitoring strategy. Journal of Volcanology and

Geothermal Research, 366, 13-26. https://doi.org/10.1016/j.jvolgeores.2018.10.001

Bromley, C., Sepulveda, F., Mannington, W., Currie, S., Abele, M. (2019) Novel Application of Continuous Gravity and Gnss to Understand Effects of Liquid Saturation Changes on Yielding Deformation. 41st New Zealand Geothermal Workshop, 1-9.

Bryan, C. J., Sherburn, S., Bibby, H. M., Bannister, S. C., Hurst, A. W. (1999). Shallow seismicity of the central Taupo Volcanic Zone, New Zealand: Its distribution and nature. New Zealand Journal of Geology and Geophysics, 42(4), 533-542. https://doi.org/10.1080/00288306.1999.9514859

Burns, B. (1997) Vegetation change along geothermal stress gradient at Te Kopia steamfield. J. R. Soc. N. Z. 27, 279-293.

Canet, C., Arana, L., González-Partida, E., Pi, T., María Prol-Ledesma, R., Franco, S. I., Villanueva-Estrada, R. E., Camprubí, A., Ramírez-Silva, G., López-Hernández, A. (2010) A statistics-based method for the short-wave infrared spectral analysis of altered rocks: An example from the Acoculco Caldera, Eastern Trans-Mexican Volcanic Belt. https://doi.org/10.1016/j.gexplo.2010.01.010

Canet, C., Hernández-Cruz, B., Jiménez-Franco, A., Pi, T., Peláez, B., Villanueva-Estrada, R. E., Alfonso, P., González-Partida, E., Salinas, S. (2015) Combining ammonium mapping and short-wave infrared (SWIR) reflectance spectroscopy to constrain a model of hydrothermal alteration for the Acoculco geothermal zone, Eastern Mexico. Geothermics, 53, 154-165. https://doi.org/10.1016/j.geothermics.2014.05.012

Claesson, L., Skelton, A., Graham, C., Dietl, C., Morth, M., Torssander, P., Kockum, I. (2004) Hydrogeochemical changes before and after major Earthquake. Geology 32, 641-644.

Chiodini, G., Cioni, R., Guidi, M., Raco, B., Marini, L. (1998). Soil CO_2 flux measurements in volcanic and geothermal areas. Applied Geochemistry, 13, 543-552. https://doi.org/10.1016/S0883-2927(97)00076-0.

Delsarte, I., Cohen, G. J. V., Momtbrun, M., Höhener, P., Atteia, O. (2021) Soil carbon dioxide fluxes to atmosphere: The role of rainfall to control CO_2 transport. Applied Geochemistry, 127. https://doi.org/10.1016/j.apgeochem.2020.104854

Deutsch, C.V. and Journel, A.G. (1998) GSLIB: Geostatistical Software Library and User's Guide. Oxford University Press, New York.

Facca, G., Tonani, F. (1967) The self-sealing geothermal field. Bulletin Volcanologique 30, 271-273. https://doi.org/10.1007/BF02597674.

Fu, C. C., Yang, T. F., Chen, C. H., Lee, L. C., Wu, Y. M., Liu, T. K., Walia, V., Kumar, A., Lai, T. H. (2017) Spatial and temporal anomalies of soil gas in northern Taiwan and its tectonic and seismic implications. Journal of Asian Earth Sciences, 149, 64-77. https://doi.org/10.1016/j.jseaes.2017.02.032

Fulignati, P., Gioncada, A., Sbrana, A. (1996) Modello geologico del sistema idrotermale- magmatico di Vulcano. In: La Volpe, L., Dellino, P., Nuccio, M., Privitera, E., Sbrana, A. (Eds.), Eds.), Progetto Vulcano. Risultati delle Attivit`a di Ricerca 1993-1995, pp. 97-118.

Ganot, Y., Dragila, M. I., Weisbrod, N. (2014) Impact of thermal convection on CO_2 flux across the earth-atmosphere boundary in high-permeability soils. Agricultural and Forest Meteorology, 184, 12-24. https://doi.org/10.1016/J.AGRFORMET.2013.09.001

Given, D.R. (1980) Vegetation on heated soils at Karapiti, Central North Island, NewZealand, and its relation to ground temperature. N. Z. J. Botan, 18, 1-13

Harvey, M., Rowland, J., Chiodini, G., Rissmann, C., Bloomberg, S., Hernandez, P., Mazot, A., Viveiros, F., Werner, C. (2018) CO_2 and Heat Release from Magmatic Hydrothermal Systems: Insights from CO_2 Flux and Other Modern Methods. Doctoral Thesis, School of Environmental Science, The University of Auckland, 126-137.

Heap, M. J., Kennedy, B. M., Farquharson, J. I., Ashworth, J., Mayer, K., Letham-Brake, M., Reuschlé, T., Gilg, H. A., Scheu, B., Lavallée, Y., Siratovich, P., Cole, J., Jolly, A. D., Baud, P., Dingwell, D. B. (2017) A multidisciplinary approach to quantify the permeability of the Whakaari/White Island volcanic hydrothermal system (Taupo Volcanic Zone, New Zealand). Journal of Volcanology and Geothermal Research, 332, 88-108. https://doi.org/https://doi.org/10.1016/j.jvolgeores.2016.12.004

Hinkle, M. E. (1991) Seasonal and geothermal production variations in concentrations of He and CO_2 in soil gases, Roosevelt Hot Springs Known Geothermal Resource Area, Utah, U.S.A. Applied Geochemistry, 6(1), 35-47. https://doi.org/10.1016/0883-2927(91)90061-S

Hopp, C., Sewell, S., Mroczek, S., Savage, M., Townend, J. (2020). Seismic response to evolving injection at the Rotokawa geothermal field, New Zealand. Geothermics, 85. https://doi.org/10.1016/j.geothermics.2019.101750

Hochstein, M.P., Bromley, C.J. (2005) Measurement of heat flux from steaming grounds. Geothermics 34, 133-160. https://doi.org/10.1016/j.geothermics.2004.04.002.

Hughes, E.C., Mazot, A., Kilgour, G., Asher, C., Michelini, M., Britten, K., Chardot, L., Feisel, Y., Werner, C., (2019) Understanding Degassing Pathways Along the 1886 Tarawera (New Zealand) Volcanic Fissure by Combining Soil and Lake CO_2 Fluxes. Frontiers in Earth Science, 7. https://doi.org/10.3389/feart.2019.00264

Henley, R. W., and Ellis, A. J. (1983) Geothermal systems ancient and modern: a geochemical review. Earth-Science Reviews, 19, 1-50. https://doi.org/https://doi.org/10.1016/0012-8252(83)90075-2

McLean, K., and Richardson, I. (2019) Greenhouse Gas Emissions from New Zealand Geothermal Power

Generation in Context. 41st New Zealand Geothermal Workshop, 1-9.

Mclean, K., Richardson, I., Quinao, J., Clark, T., Owens, L., Zealand, N., Tuwharetoa, N., Assets, G. (2020) Greenhouse Gas Emissions from New Zealand Geothermal: Power Generation and Industrial Direct Use. 42nd New Zealand Geothermal Workshop, 1-8.

Mclean, K., and Richardson, I. (2021) Geothermal Greenhouse Gas Emissions in New Zealand in 2020: Lifecycle and Operational Emissions. 43rd New Zealand Geothermal Workshop, 1-8.

New Zealand Geothermal Association (2022 Retrieved from: https://www.nzgeothermal.org.nz/

Sbrana, A., Lenzi, A., Paci, M., Gambini, R., Sbrana, M., Ciani, V., Marianelli, P. (2021) Analysis of natural and power plant CO_2 emissions in the mount amiata (Italy) volcanic-geothermal area reveals sustainable electricity production at zero emissions. Energies, 14(15). https://doi.org/10.3390/en14154692

Seward, A., Ashraf, S., Reeves, R., Bromley, C. (2018). Improved environmental monitoring of surface geothermal features through comparisons of thermal infrared, satellite remote sensing and terrestrial calorimetry. Geothermics 73, 60-73. https://doi.org/10.1016/j.geothermics.2018.01.007.

Sheppard, D., Mroczek, E. (2002) CO_2 Fluxes from geothermal systems: Accessing the effects of Exploitation and the Carbon Tax implications. 24th New Zealand Geothermal Workshop, 1-5.

Rissmann, C., Christenson, B., Werner, C., Leybourne, M., Cole, J., Gravley, D. (2012) Surface heat flow and CO2 emissions within the Ohaaki hydrothermal field, Taupo Volcanic Zone, New Zealand. Applied Geochemistry, 27(1), 223-239. https://doi.org/10.1016/J.APGEOCHEM.2011.10.006

Rosenberg, M. D., Wilson, C. J. N., Bignall, G., Ireland, T. R., Sepulveda, F., Charlier, B. L. A. (2020) Structure and evolution of the Wairakei-Tauhara geothermal system (Taupo Volcanic Zone, New Zealand) revisited with a new zircon geochronology. Journal of Volcanology and Geothermal Research, 390, 1-21. https://doi.org/10.1016/j.jvolgeores.2019.106705

Taussi, M., Brogi, A., Liotta, D., Nisi, B., Perrini, M., Vaselli, O., Zambrano, M., Zucchi, M. (2022) CO_2 and heat energy transport by enhanced fracture permeability in the Monterotondo Marittimo-Sasso Pisano transfer fault system (Larderello Geothermal Field, Italy). Geothermics, 105, 102531. https://doi.org/10.1016/J.GEOTHERMICS.2022.102531

The National Climate Database, 2022. NIWA, Auckland, New Zealand. Retrieved from: https://cliflo.niwa.co.nz/

Van Manen, S.M., Reeves, R.R. (2012) An Assessment of Changes in Kunzea ericoidesvar.microflora and other hydrothermal vegetation at the Wairakei-Tauhara Geothermal Field, New Zealand. Environ. Manage. 50, 766-786

Wang, J., Epstein, H. E., Wang, L. (2010). Soil CO_2 flux and its controls during secondary succession. Journal of Geophysical Research: Biogeosciences, 115(2). https://doi.org/10.1029/2009JG001084

Werner, C., Hochstein, M., Bromley, C. (2004). CO_2-flux of Steaming Ground at Karapiti, Wairakei. 26th New Zealand Geothermal Workshop, 1-6.

WestSystems. (2019) Portable diffusive flux meter LI820 carbon dioxide handbook. Retrieved from: https://www.westsystems.com/wp-content/uploads/2019/01/Handbook_Portable_9.1.pdf

Yang, T.F., Fu, C.C., Walia, V., Chen, C.-H., Chyi, L.L., Liu, T.K., Song, S.R., Lee, M., Lin, C. W., Lin, C.C. (2006) Seismo-geochemical variations in SW Taiwan: multi- parameter automatic gas monitoring results. Pure Appl. Geophys. 163, 693-709.